ISEIS

Journal of Environmental Informatics 38(2) 145-161 (2021)

Journal of Environmental Informatics

www.iseis.org/jei

Development of An Integrated Method (MGCMs-SCA-FER) for Assessing the Impacts of Climate Change – A Case Study of Jing-Jin-Ji Region

H. Mei[1, 2], Y. P. Li[1, 3 *], J. Lv[4], X. J. Chen[3], C. Lu[3], C. Suo[4], and Y. Ma[1]

[1] *Environment and Energy Systems Engineering Research Center, School of Environment, Beijing Normal University, Beijing 100875, China*
[2] *Shenzhen Academy of Environmental Sciences, Shenzhen 518001, China*
[3] *Institute for Energy, Environment and Sustainable Communities, University of Regina, Regina, SK S4S 0A2, Canada*
[4] *Sino-Canada Energy and Environmental Research Academy, North China Electric Power University, Beijing 102206, China*

Received 20 March 2020; revised 26 April 2020; accepted 23 June 2020; published online 03 January 2021

ABSTRACT. In this study, an integrated method (abbreviated as MGCMs-SCA-FER) is developed for assessing the impacts of climate change, which incorporates multiple global climate models (MGCMs), stepwise cluster analysis (SCA), and fixed-effects regression (FER) within a general framework. MGCMs-SCA-FER is capable of (i) dealing with the uncertainty in climate change projection caused by heterogeneity of structures and parameters of GCM; (ii) capturing nonlinear relationship between input variables and outputs without assumption of their functions; (iii) identifying interaction of different units and quantifying the effects of climate change on electricity demand. MGCMs-SCA-FER is then applied to Jing-Jin-Ji for assessing the impacts of climate change on single-city and entire-region electricity demands. Results demonstrated that climate change projections and electricity demand predictions varied significantly across different GCMs and RCPs. Results disclose that (i) Jing-Jin-Ji region would experience a warmer climate in the next 80 years of 2021 ~ 2100 (For every decade, temperatures would increase by [0.17, 0.23] °C under RCP4.5 and [0.35, 0.54] °C under RCP8.5); (ii) For 1 °C increase in temperature, annual electricity demand would rise by 4.5%; (iii) electricity intensity has the most significant impact on electricity demand for Jing-Jin-Ji region; (iv) electricity demand would increase under all scenarios, and the electricity demand under RCP8.5 would be higher than that under RCP4.5. From a long-term perspective, analyzing the climate change impacts on electricity demand and making adaptive management strategy are important for the regional sustainability.

Keywords: climate change, electricity demand, fixed-effects regression, impact assessment, multi-GCMs, stepwise cluster analysis

1. Introduction

Due to a large amount of greenhouse gases (GHGs) emission, climate change has been evident worldwide with 0.85 °C increase of an average surface air temperature from 1880 to 2012 (IPCC, 2013). As one of the most pressing issues in the world, climate change has caused evident impacts on natural and human systems (e.g., agriculture, forestry, mining, manufacturing, transportation and energy). For energy systems planning, electricity demand has obvious response to climate change since global warming can affect heating and cooling loads such as air conditioner, refrigerator and water heater (Jylhä et al., 2015; Invidiata and Ghisi, 2016; Ji et al., 2020; Dong et al., 2021). The rising temperature can result in increased demand for cooling in hot weather but decrease demand for heating in cold weather (AL-Musaylh et al., 2019; Mukherjee et al., 2019). Climate change is likely to be predictable over the next century, due to consistently growing GHGs emissions. The global temperature would increase 0.3 ~ 4.8 °C (relative to 1986 ~ 2005 level) by the end of 21th (Ang et al., 2017). As the leading contributor of GHGs, electric-power sector is largely driven by thermal technology throughout the world, generating over one-third of the global energy-related carbon dioxide (CO_2) emissions (Zeng et al., 2011; Jin et al., 2017). On the other hand, electricity demand is expected to increase in the future due to the rapid development of economy and the significant improvement of people's living standards, particularly for some developing countries (e.g., China and India) (Fan et al., 2019; Lv et al., 2020; Fu et al., 2021). Therefore, it is essential to assess the effects of climate change on electricity demand and understand the response of electric power system to future climate change.

Previously, a number of research works were conducted for investigating the impacts of climate change on electric power system (especially for electricity demand) (Zeng et al., 2011; Dong et al., 2012). Emodi et al. (2018) employed an auto-regression distributed lag model to analyze the short- and long-term impacts of climate change on electricity demand in Australia; results indicated that electricity consumption would increase due to rising temperature. Alberini et al. (2019) adopted a fixed-effects regression (FER) model with hourly electricity demand in Italian to examine the sensibility of residential electricity demand to temperature; results discovered that the electricity demand would increase sharply with temperature rising

* Corresponding author. Tel.: +86 10 58800156; Fax: +86 10 58800156.
E-mail address: yongping.li@iseis.org (Y. P. Li).

ISSN: 1726-2135 print/1684-8799 online
 doi:10.3808/jei.202100458

when temperature exceeds 24.4 °C. Burillo et al. (2019) forecasted peak electricity demand for Los Angeles County under RCP4.5 and RCP8.5 (i.e., representative concentration pathway scenarios 4.5 and 8.5, respectively); results showed that the peak demand will increase 25.5% by 2060 and 6.0% of the growth is caused by climate change. Mei et al. (2020) incorporated different GCMs within a support vector regression model to predict future electricity demand in China; results revealed that the national electricity demand would increase about 58.6% from 2021 to 2050. Zheng et al. (2020) quantified the effects of climate change on total electricity consumption (TEC) and residential electricity consumption (REC) for Guangzhou (in China) based on different GCMs and emission scenarios; results showed that city's TEC and REC would respectively increase by 3.2 ~ 10.4% and 1.1 ~ 3.5%, compared with the baseline period of 1986 ~ 2005. In general, the previous studies mainly focused on establishing the response relationship between climate change and electricity demand, some of which can further predict the future electricity demand directly based on the outputs of GCMs; downscaling techniques for acquiring high-resolution climate scenarios during the impacts assessment of climate change on electricity demand at regional scale were rarely conducted.

In fact, the coarse spatial resolutions of large-scale simulation outputs of GCMs are hundreds of kilometers, resulting in it difficult to accurately reflect local-scale climate change and further leading to deviations for the impacts assessment of climate change on electricity demand at regional scale (Ayar et al., 2016; Zhuang et al., 2018; Zhai et al., 2021). Stepwise clustering analysis (SCA) has strongly flexibility in dealing with discrete and nonlinear problems through describing the complex relationships between inputs and outputs as clustering trees rather than function expressions (Qin et al., 2007). Previously, SCA was employed to some complex practical problems, such as climate projection, runoff simulation, and environmental analysis. Wang et al. (2013) proposed a statistical downscaling tool (based on SCA technique) to obtain 10 km daily mean temperature and monthly precipitation projections for Toronto, Canada; results indicated that the observed temperature and precipitation in the validation period can be well reproduced by SCA. Zhuang et al. (2017) employed SCA technique to evaluate climate change impacts on the hydrology of watershed in northwestern China, implying that SCA is capable of downscaling climate projections for different stations and helping understand the spatial heterogeneity of climate change. Zhai et al. (2019) utilized SCA to investigate the plausible changes in daily maximum, minimum, and mean temperatures in Ottawa under multiple scenarios; results showed that the SCA method had excellent performance in future climate change projections. Generally, the previous works showed that SCA is an effective tool for climate scenarios downscaling; unfortunately, few of them extended the downscaled results from SCA to analyze the impacts of climate change on regional electricity demand.

Another challenge faced by the impact assessment is inherent uncertainty of GCM. Due to the differences in driving mechanisms and boundary conditions of GCMs, climate scenarios vary among different GCMs (Perez et al., 2014; Mei et al., 2020). Since one GCM cannot reflect such an uncertainty, multiple global climate models (MGCMs) are desired to be incorporated in downscaling model framework to reflect the inherent uncertainty of GCM and mitigate the influence of uncertainty on electricity demand (Li et al., 2010; Souvignet and Heinrich, 2011; Zhuang et al., 2017; Su et al., 2021). Moreover, interaction of different units exists in the process of accessing the effects of climate change on electricity demand at a regional scale. Fixed-effects regression (FEG, based on panel data) has advantages in dealing with such an interaction of different units during quantifying the effects of climate change on electricity demand (Asadoorian et al., 2008). Nevertheless, no previous study was reported for analyzing the impacts of climate change on regional-scale electricity demand, through incorporating techniques of MGCMs, SCA and FEG within a general framework.

This study aims to develop an integrated method (abbreviated as MGCMs-SCA-FER) for assessing the climate change impacts on regional-scale electricity demand, through incorporating multiple global climate models (MGCMs), stepwise cluster analysis (SCA), and fixed-effects regression (FER). The novelty and contribution of this study are: (i) an integrated MGCMs-SCA-FER method is firstly advanced for analyzing climate change impacts, which is superior to the traditional approaches; (ii) it can deal with the uncertainty in climate change projection caused by heterogeneity of structures and parameters of GCM; (iii) it is capable of generating high-resolution climate projections, investigating the impacts of climate change on electricity demand and further predicting future electricity demand; (iv) it is the first attempt at applying MGCMs-SCD-FER to analyze the impacts of climate change on electricity demand in Jing-Jin-Ji region under multiple scenarios; (v) results of future climate change projections, climate change impacts on electricity demand, as well as future electricity demand prediction can be generated, which will provide decision support for policymakers.

2. Methodology

The MGCMs-SCA-FER method is consisted of (i) climate data extracted from MGCMs, (ii) regional-scale climate scenarios downscaled by SCA, and (iii) electricity demand predicted by FER. The general flow chart is shown in Figure 1. In detail, the daily gridded data are extracted from MGCMs (i.e., CanESM2, CNRM-CM5 and NorESM1-M); the daily gridded data are used to drive SCA downscaling model to generate regional-scale synthetic daily time series of climate variables [i.e., maximum temperature (Tmax), minimum temperature (Tmin), and mean temperature (Tmean)]; various climate scenarios are employed as inputs of FER to investigate climate change impacts on electricity demand and then predict future electricity demand.

Climate scenarios projected by single GCM are subject to significant uncertainty because of the various driving mechanisms and boundary conditions in GCM experiments. MGCMs can compared with each other for helping decision makers better understand the uncertainties in climate change projections. According to literature survey, three popular GCMs [i.e., CanESM2 (CA), CNRM-CM5 (CN) and NorESM1-M (NO)] and two climate scenarios (i.e. RCP4.5 and 8.5) are considered (Hou et al., 2019; Sun et al., 2019). The National Centers for Envi-

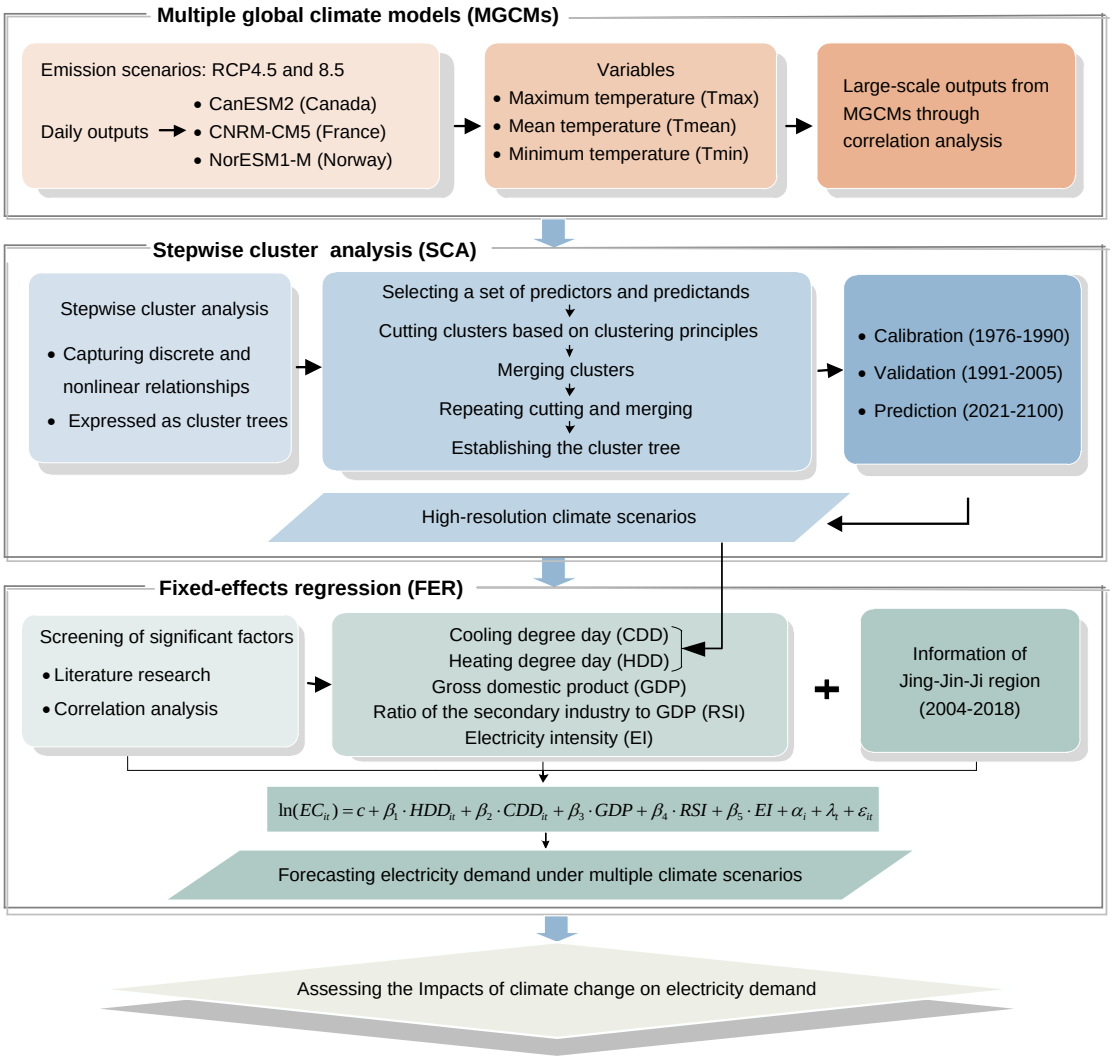

Figure 1. Framework of MGCMs-SCA-FER.

ronment and Prediction (NCEP) reanalysis data are employed for assisting in establishing the relationship among GCMs outputs with the observed data. The spatial resolutions and institutions of GCMs and NECP reanalysis data are listed in Table 1.

SCA is used for downscaling (converting the large-scale atmospheric variables into the local climate variables) through capturing discrete and nonlinear relationship (expressed as cluster trees) between large-scale atmospheric variables (i.e., predictors) from MGCMs and climate variables (i.e., predictands) from meteorological stations. The essence of SCA is to form a classification tree through a series of cutting or merging processes based on a given statistical standard (Huang et al., 2006). The detailed steps are: (i) selecting a set of predictors and predictands, (ii) cutting of clusters based on clustering principles, (iii) merging of clusters, (iv) repeating cutting-mergence until no cluster can be cut and merged, (v) establishing the cluster tree from the training samples, and (vi) generating the local-scale climate scenarios. The detailed principle of SCA method is provided in the Appendix to this paper.

Table 1. GCMs and NECP Reanalysis Data

GCM	Institute	Grid resolution (latitude × longitude, deg)
CanESM2 (CA)	Canadian Centre for Climate Modelling and Analysis, Canada	2.79 × 2.81
CNRM-CM5 (CN)	Centre Europeen de Recherche et de Formation Avancee en Calcul Scientifique, France	1.40 × 1.41
NorESM1-M (NO)	Norwegian Climate Centre, Norway	1.90 × 2.50
NECP	NOAA National Center for Environmental Prediction, USA	2.50 × 2.50

In this study, five large-scale predictor variables (i.e., surface temperature, near-surface air temperature, air temperature at 700 hpa, air temperature at 700 hpa, and geopotential height at 250 hpa) were screened out through correlation analysis between 30 predictors and the predictands (i.e., Tmax, Tmin and

Tmean) (Mtongori et al., 2016; Zhou et al., 2018). The observed data for Tmax, Tmin and Tmean and NCEP reanalysis data for five predictors (during 1976 ~ 1990) were employed for calibrating SCD model. The simulation outputs of three GCMs for five predictors (in 1991 ~ 2005) were input into the calibrated model to generate the simulated values of station-based Tmax, Tmin and Tmean. The simulated values were compared with the observed data for validation purposes, which can be evaluated by determination coefficient (R^2). The criteria are defined as follows:

$$R^2 = \frac{\left(n\sum_{i=1}^{n} obs_i \cdot pre_i - \sum_{i=1}^{n} obs_i \cdot \sum_{i=1}^{n} pre_i\right)^2}{\left[n\sum_{i=1}^{n}(obs_i)^2 - \left(\sum_{i=1}^{n} obs_i\right)^2\right]\left[n\sum_{i=1}^{n}(pre_i)^2 - \left(\sum_{i=1}^{n} pre_i\right)^2\right]} \quad (1)$$

where obs_i is the observed data value on day i; pre_i is the predicted data value on day i; and obs_i is the mean observed data value; n is the number of simulated days. The closer R^2 value to 1, the model performance is better. Finally, the simulation outputs of three GCMs in 2021 ~ 2100 were employed to drive the calibrated model to project future climate scenarios.

In this study, five factors are selected for predicting electricity demand, including two climatic variables [i.e., cooling degree day (CDD) and heating degree day (HDD)] and three socioeconomic variables [i.e., gross domestic product (GDP), ratio of the output value of the secondary industry to the GDP (RSI), and electricity intensity (EI)] (Ahmed et al., 2012; Zheng et al., 2020). CDD and HDD are employed to quantify heating demand and cooling demand, respectively, calculated by the downscaled Tmax and Tmin (Craig and Feng, 2016). The annual CDD and HDD are defined as follows:

$$CDD = \sum_{i=1}^{n} \alpha_c (T_i - T_b),\ \alpha_c = \begin{cases} 1 & if\ T_i - T_b > 0 \\ 0 & if\ T_i - T_b < 0 \end{cases} \quad (2a)$$

$$CDD = \sum_{i=1}^{n} \alpha_c (T_i - T_b),\ \alpha_c = \begin{cases} 1 & if\ T_i - T_b > 0 \\ 0 & if\ T_i - T_b < 0 \end{cases} \quad (2b)$$

where n is the total number of days in a year; T_b is balance point temperature and 18 °C is regarded as the point temperature in this study (Fan et al., 2019); T_i is the daily average temperature on day i. RSI can be calculated by GDP and output value of secondary industry. EI can be calculated by electricity consumption and GDP.

Then, panel data are employed to establish regression relationship between electricity demand and influencing factors (i.e., CDD, HDD, GDP, RSI and EI). Panel data can combine time series with cross-sections to enhance the quality and quantity of data, better than using only one of these two dimensions; panel data can also reduce the collinearity among multiple variables, leading to estimation results more effective, stable and reliable. The mixed regression (MR), fixed-effects regression (FER) and random-effects regression (RER) method are commonly employed for panel data analysis (Yaffee, 2003). In this study, the null hypothesis is rejected at the 1% significance level according to the results of the F-test, representing that FER is appropriate to be used rather than MR; the null hypothesis is rejected at the 1% significance level based on the results of the Hausman test, meaning that FER should be chosen rather than RER. FER have constant slopes but different intercepts. The intercepts would differ with individuals and with time. FER can estimate the effects of cross section and time series separately, and thus more accurate interpretations of the dependent variables can be obtained. Based on the panel data, a fixed-effect regression (FER) model is constructed to analyze the impacts of climate change on electricity demand. The FER model is defined as:

$$\ln(EC_{it}) = c + \beta_1 \cdot HDD_{it} + \beta_2 \cdot CDD_{it} + \beta_3 \cdot GDP + \beta_4 \cdot RSI + \beta_5 \cdot EI + \alpha_i + \lambda_t + \varepsilon_{it} \quad (3)$$

where i is the city (or province); t is the time series; $\ln(EC_{it})$ is the logarithmic variable of electricity consumption at region i and time t; c is the intercept term. HDD and CDD are climatic variables; GDP, RSI and EI are socioeconomic variables; β_i (i = 1, 2 …, 5) are regression coefficients for each variable; α_i is the regional fixed effect, reflecting the regional individual differences; λ_t is the temporal point fixed effect, reflecting the temporal difference; ε_{it} is the random error term.

3. Case Study

3.1. Statement of Problem

Jing-Jin-Ji region is the capital circle of China, including two municipalities (Beijing and Tianjin) and one province (Hebei), as shown in Figure 2. This region covered an area of 216 × 10^3 km^2 and hosted a population of 112.8 million in 2018. In the past twenty years, the regional gross domestic product (GDP) increased rapidly with an annual growth rate of 12.9%, reaching 8,514 billion RMB¥ and occupying 9.5% of total national GDP in 2018 (CSY, 2018; Cai et al., 2019). Due to the rapid industrialization and urbanization, the regional electricity consumption has risen sharply. From 2009 to 2017, Electricity consumption of Beijing, Tianjin and Hebei increased by 177.5, 240.6 and 325.3%, respectively (reaching 106.7 × 10^9, 80.6 × 10^9 and 344.1 × 10^9 kWh in 2017). In 2017, the electricity-generation capacities of Beijing, Tianjin and Hebei were 38.8 × 10^9, 61.1 × 10^9 and 281.7 × 10^9 kWh, respectively; this implies that the domestic electricity generation cannot afford the local electricity demand, especially for Beijing (HEY, 2018; TSY, 2018; BSY, 2019). More electricity was imported from surrounding provinces (e.g., Neimenggu, Shanxi and Jilin) to Jing-Jin-Ji region. In addition, the per capita electricity consumption in Jing-Jin-Ji region is still much lower than those in many developed countries. In 2018, per capita electricity consumption in Jing-Jin-Ji region was 5025.8 kWh, while per capita electricity consumptions in Canada and USA respectively were 17657.9 and 13634.5 kWh, which were 3.5 times and 2.7 times of that in Jing-Jin-Ji region.

Accompanying with the further socioeconomic development, electricity demand in Jing-Jin-Ji region will continue to

increase in the future, imposing a great challenge of balancing electricity demand and electricity supply. In order to alleviate air pollution and mitigate climate change, electricity generation from the renewable energy will gradually rise and transfer towards a clean-production and low-carbon pattern. Jing-Jin-Ji region has implemented the policy of shifting from coal to electricity due to the short of raw materials and the pressure of environmental control. More and more electrification industries (e.g., electric vehicles) are emerging; as a consequence, the share of electricity consumption to total energy consumption will increase with time. In addition, climate change is likely to be predictable over the next century, due to consistently growing GHGs emission. In the future, Climate change will have more obvious impacts on cooling and heating demands as climate warming intensifies. The improvement of economy level will also promote people to increase the utilization rate of air conditioning, refrigerator and electric water heater, which will further amplify the impacts of climate change on electricity demand. It is nec-essary for decision makers to predict the future electricity demand precisely under changing climate for meeting the regional electricity demand and effectively avoiding excess capacity or loss of electricity transmission.

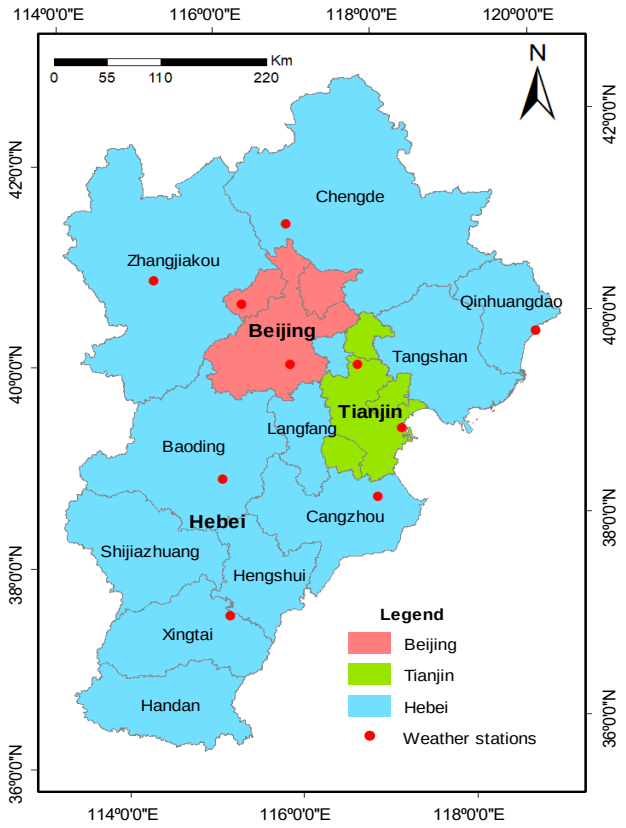

Figure 2. The study area.

3.2. Data Collection and Processing

The observed daily data of three temperature variables (i.e., Tmax, Tmin and Tmean) of ten meteorological stations (as shown in Table 2) from 1976 to 2018 were download from National Meteorological Information Center (http://data.cma.cn/, accessed January 15, 2020). In order to construct the relationship between predictors (GCM outputs) with predictands (observed data), the daily simulation outputs of the National Centers for Environment and Prediction (NCEP) Reanalysis Products from 1976 to 2005 were download from Physical Science Division of Earth System Research Laboratory (https://www.esrl.noaa.gov/psd/data/gridded/data.ncep.reanalysis.html, accessed January 24, 2020). Daily simulation outputs of GCMs were obtained from Coupled Model Intercomparison Project 5 (CMIP5) dataset archive (https://esgf-node.llnl.gov/projects/cmip5/, accessed January 25, 2020). The historical period is 1976 ~ 2005 and the future period is 2021 ~ 2100. Some socioeconomic data (i.e., population and GDP, out- put value of secondary industry) and the amount of electricity consumption of Jing-Jin-Ji region in 2004 ~ 2018 were collected from the National Bureau of Statistics and related statistical yearbooks. According to Shared Socioeconomic Pathways, the data of population and GDP in 2021 ~ 2100 of China were obtained and then that of Jing-Jin-Ji region can be estimated by empirical formula (https://tntcat.iiasa.ac.at/SspDb/dsd?Action=htmlpage&page=about, accessed February 12, 2020). RSI and EI of Jing-Jin-Ji region in 2021 ~ 2100 were estimated from governmental reports and literature references.

Table 2. Description of Ten Meteorological Stations

Meteorological stations	Geographical coordinates (latitude, longitude)	Province/city
Beijing	(39.8°N, 116.5°E)	Beijing
Yanqing	(40.5°N, 116.0°E)	Beijing
Baodi	(39.7°N, 117.3°E)	Tianjin
Tanggu	(39.1°N, 117.8°E)	Tianjin
Zhangjiakou	(40.8°N, 114.9°E)	Hebei
Qinhuangdao	(39.9°N, 119.5°E)	Hebei
Baoding	(38.7°N, 115.5°E)	Hebei
Huangye	(38.4°N, 117.3°E)	Hebei
Fengning	(41.2°N, 116.6°E)	Hebei
Nangong	(37.4°N, 115.4°E)	Hebei

4. Result and Discussion

4.1. Temperature Projections

Based on SCA technique, three temperature variables (Tmean, Tmax and Tmin) were put together to build a training model due to the same predictors (i.e., time series of surface temperature, near-surface air temperature, air temperature at 700 hpa, air temperature at 700 hpa, and geopotential height at 250 hpa). After training a total of 27,395 calibration samples (in 1976 ~ 1990), a cluster tree was generated for daily Tmax, Tmin and Tmean of a meteorological station. In this study, ten cluster trees of the selected ten meteorological stations were obtained. Figure 3 shows the cluster tree for Beijing's meteorological station in the calibration period (1976 ~ 1990). The criterion for cutting and emerging clusters is $P < 0.01$ and $P > 0.01$, respectively. The P values represent the significance levels of F test, and $P < 0.01$ implies that there is a highly significant difference between two clusters. When ten cluster trees

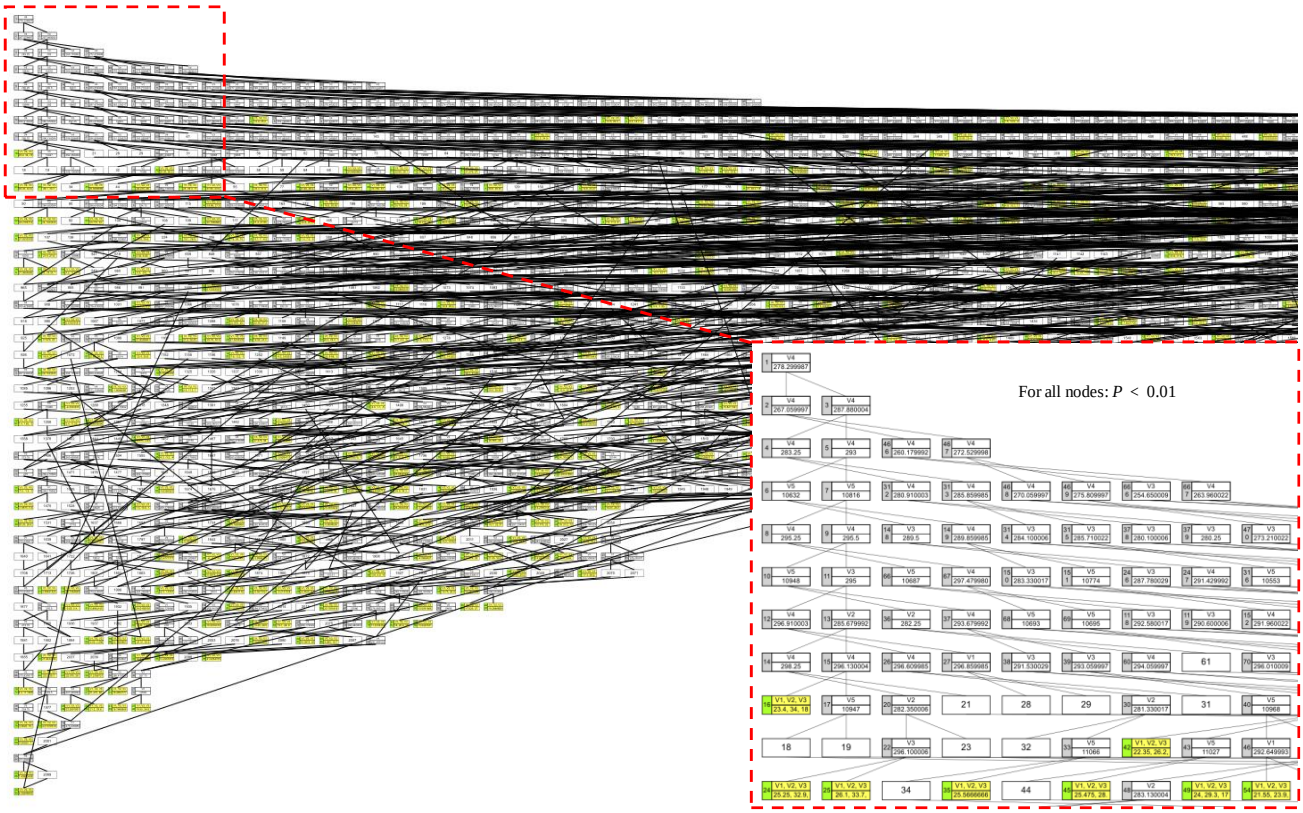

Figure 3. The cluster tree for Beijing's meteorological stations (1976 ~ 1990).

were generated, the simulation outputs of MGCMs could be employed for driving the downscaling models to generate future climate change scenarios for Jing-Jin-Ji region.

Figures 4 and 5 present the monthly observed and simulated values (Tmean, Tmax and Tmin) of Jing-Jin-Ji region from MGCMs during the validation period (1991 ~ 2005). The results show that all statistical values of R^2 would be no less than 0.92, most of which are between 0.95 and 0.97. This means that SCA is capable of downscaling climate projections for the ten stations. In detail, the minimum R^2 of 0.923 is associated with the simulated Tmax for Nangong meteorological station (in Hebei) from CNRM-CM5 (CN); the maximum R^2 of 0.974 is associated with the simulated Tmin for Fengning meteorological station (in Hebei) from NorESM1-M (NO). High R^2 values indicate that there would be high agreements between observed and simulated Tmean, Tmax and Tmin. Results reveal that SCA can effectively capture the discrete and nonlinear relationships between predictors and predictands.

Figures 6 to 8 present the results of monthly Tmean, Tmax and Tmin (for Beijing, Tianjin and Hebei) projected from MGCMs under different emission scenarios (2021 ~ 2100), respectively. The results indicate that Tmean, Tmax and Tmin (for Beijing, Tianjin and Hebei) under RCP4.5 and RCP8.5 would increase in the next 80 years. For Beijing, Tmean, Tmax and Tmin would increase by [0.18, 0.20], [0.18, 0.20] and [0.18, 0.20] °C per decade under RCP4.5, and rise by [0.40, 0.46], [0.40, 0.46] and [0.42, 0.46] °C per decade under RCP8.5. For Tianjin, Tmean, Tmax and Tmin would increase by [0.18, 0.22], [0.18, 0.20] and [0.18, 0.23] °C per decade under RCP4.5, and rise by [0.40, 0.50], [0.38, 0.47] and [0.41, 0.50] °C per decade under RCP8.5. For Hebei, Tmax, Tmin and Tmean would climb by [0.19, 0.22], [0.17, 0.20] and [0.19, 0.23] °C per decade under RCP4.5, and increase by [0.38, 0.52], [0.35, 0.47] and [0.41, 0.54] °C per decade under RCP8.5. Summarily, results indicated that the increase amplitudes of Tmean, Tmax and Tmin would different. For Jing-Jin-Ji region, Tmin would have the largest increase and Tmax would increase the least in the next 80 years. This also means that climate change would have a more significant impact on the cold weather compared with the hot weather.

Figures 5 to 7 also show that different GCMs and RCPs would lead to varied projections of future Tmean, Tmax and Tmin. The rates of temperature (Tmean, Tmax and Tmin) increases under RCP8.5 would be higher than those under RCP4.5. This is due to the factors: (i) CO_2 concentration in the atmosphere under RCP8.5 is assumed to be higher than that under RCP4.5, and (ii) higher CO_2 concentration can lead to faster global warming. Projected Tmax, Tmin and Tmean from different GCMs would vary. For Beijing, Tmean projected from NorESM1-M would be 1.40 °C higher than that from CNRM-CM5 and 2.45 °C lower than that from CanESM2. This can be attributed to the uncertainty of climate models, which is related to the fact that different physical and numerical formulations adopted by MGCMs can lead to different responses. Results also demonstrate that it is necessary to utilize multiple GCMs and

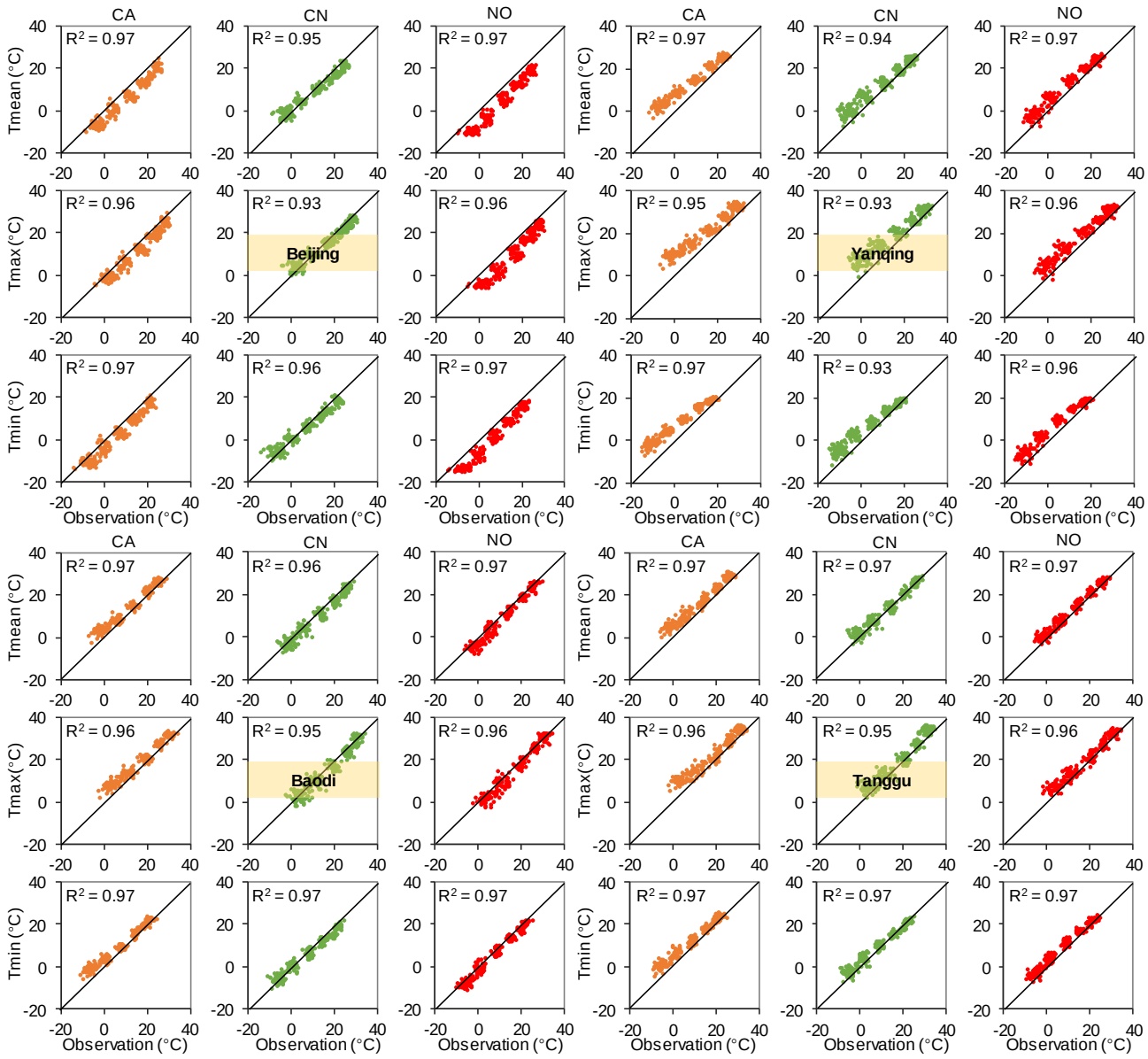

Figure 4. Validation results for monthly Tmean, Tmax, and Tmin of Beijing and Tianjin (1991 ~ 2005).

RCPs to generate future temperature projections.

4.2. Impacts on Electricity Demand

Figure 9 displays the results of annual CDD and HDD (for Beijing, Tianjin and Hebei) during the historical period (1989 ~ 2018) and the future period (2021 ~ 2100). The cooling demand (expressed as CDD) mainly appeared from May to September (around 153 days in one year), and the heating demand (expressed as HDD) mainly occurred from January to April and from October to December (around 212 days in one year). During 1989 ~ 2018, annual CDD values for Beijing, Tianjin and Hebei increased by 73.3, 58.9 and 35.1°C d per decade, respectively; annual HDD values for Beijing, Tianjin and Hebei decreased by 66.8, 41.6 and 20.4 °C d per decade, respectively. For Jing-Jin-Ji region, under RCP4.5 and RCP8.5, CDD would continue to rise and HDD would keep dropping in 2021 ~ 2100. The variation ranges of CDD and HDD under RCP8.5 would be larger than those under RCP4.5; this is because the increase of Tmean under RCP8.5 would be higher than that under RCP4.5.

Based on the panel data, the FER model was established for analyzing the impacts of climate change on the electricity demand in Jing-Jin-Ji region, and results are listed in Table 3. Both CDD and HDD play a positive role in the regional electricity demand (at 1% significance level). Since electricity demand is in natural logarithmic form, the regression coefficients of variables (e.g., CDD, HDD and GDP) should be multiplied by 100 to obtain their percentage effects on electricity demand. One unit change in CDD and HDD can alter electricity demand

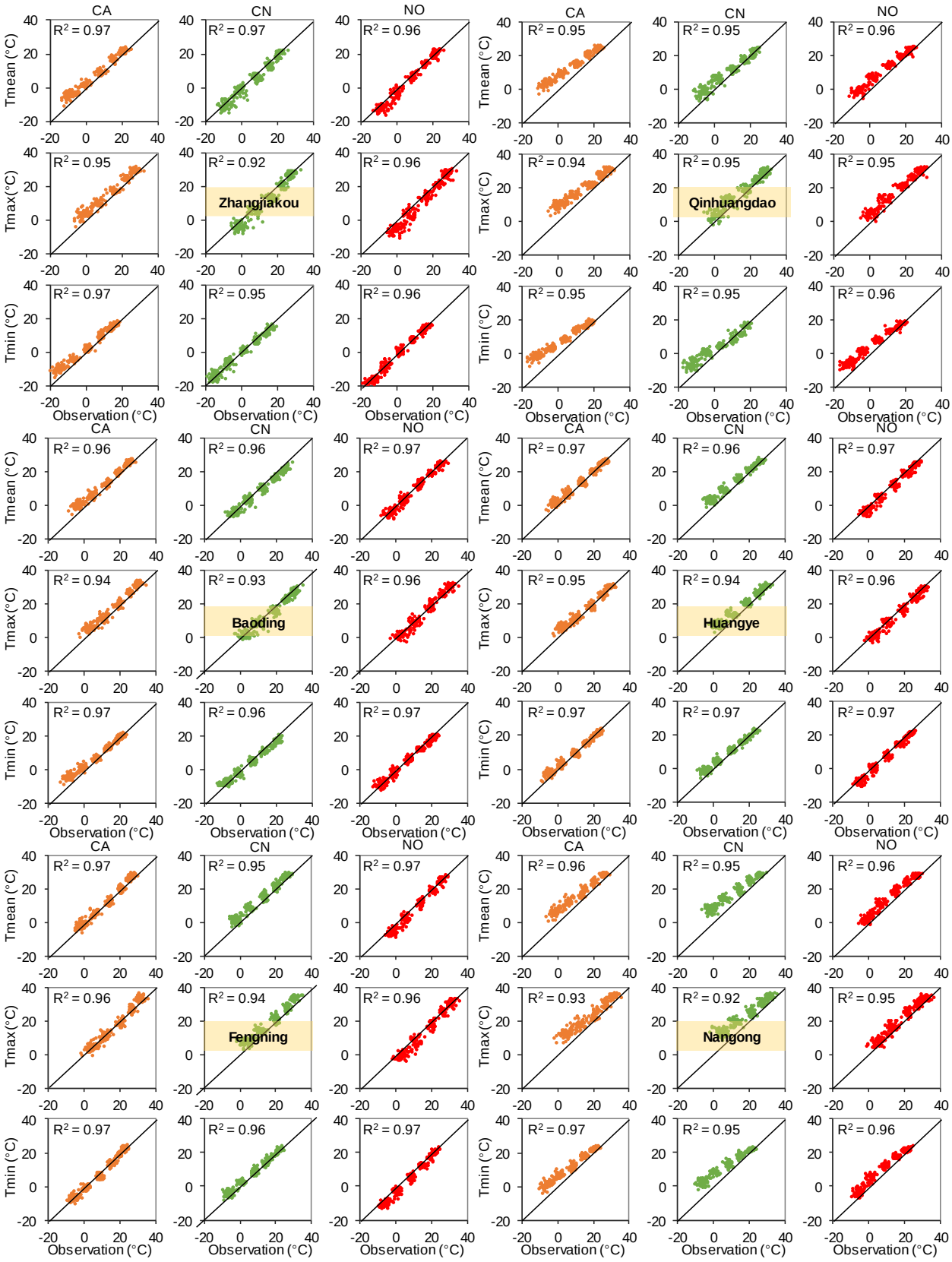

Figure 5. Validation results for monthly Tmean, Tmax, and Tmin of Hebei (1991 ~ 2005).

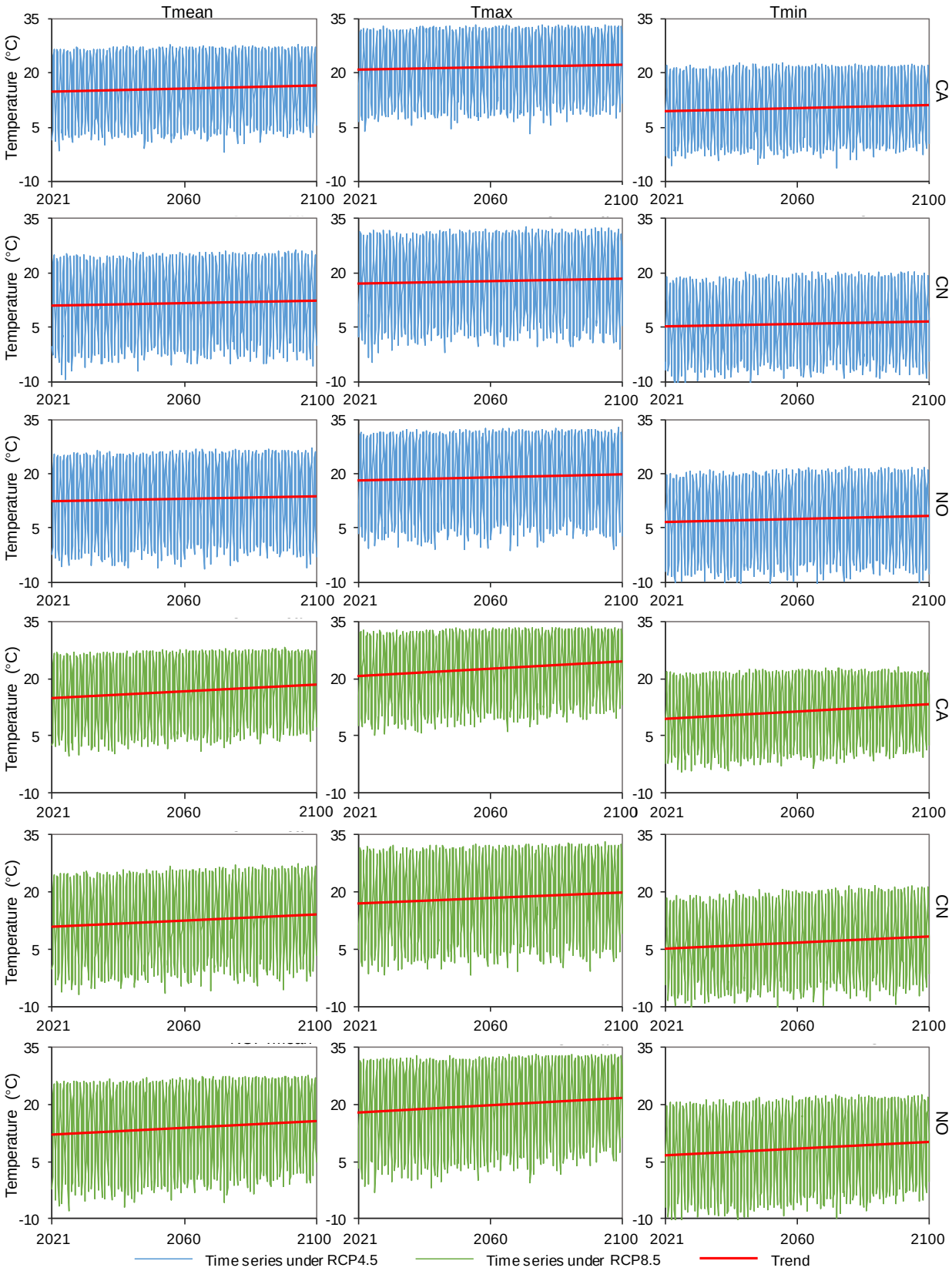

Figure 6. Projected monthly Tmean, Tmax, and Tmin of Beijing (2021 ~ 2100).

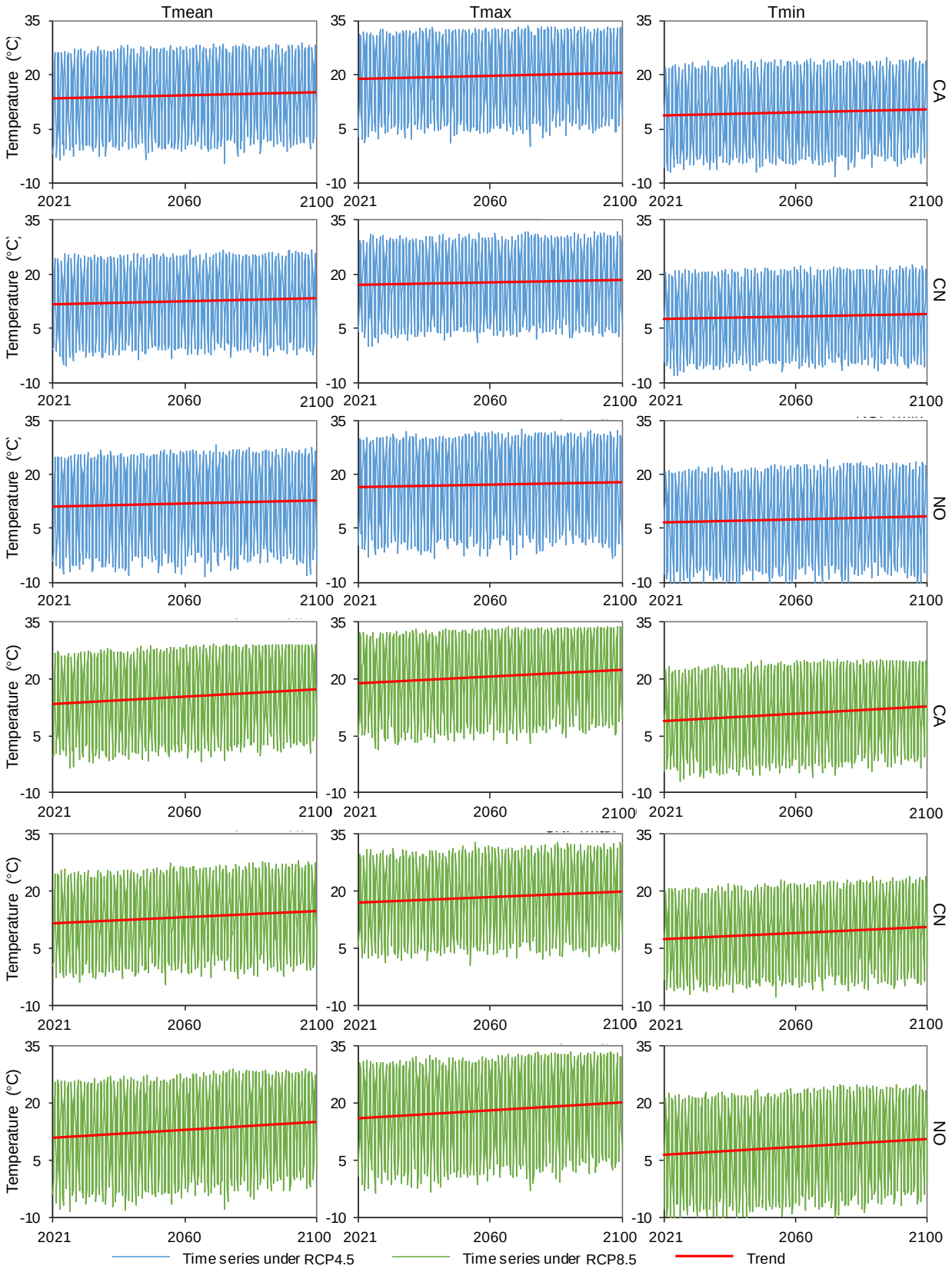

Figure 7. Projected monthly Tmean, Tmax, and Tmin of Tianjin (2021 ~ 2100).

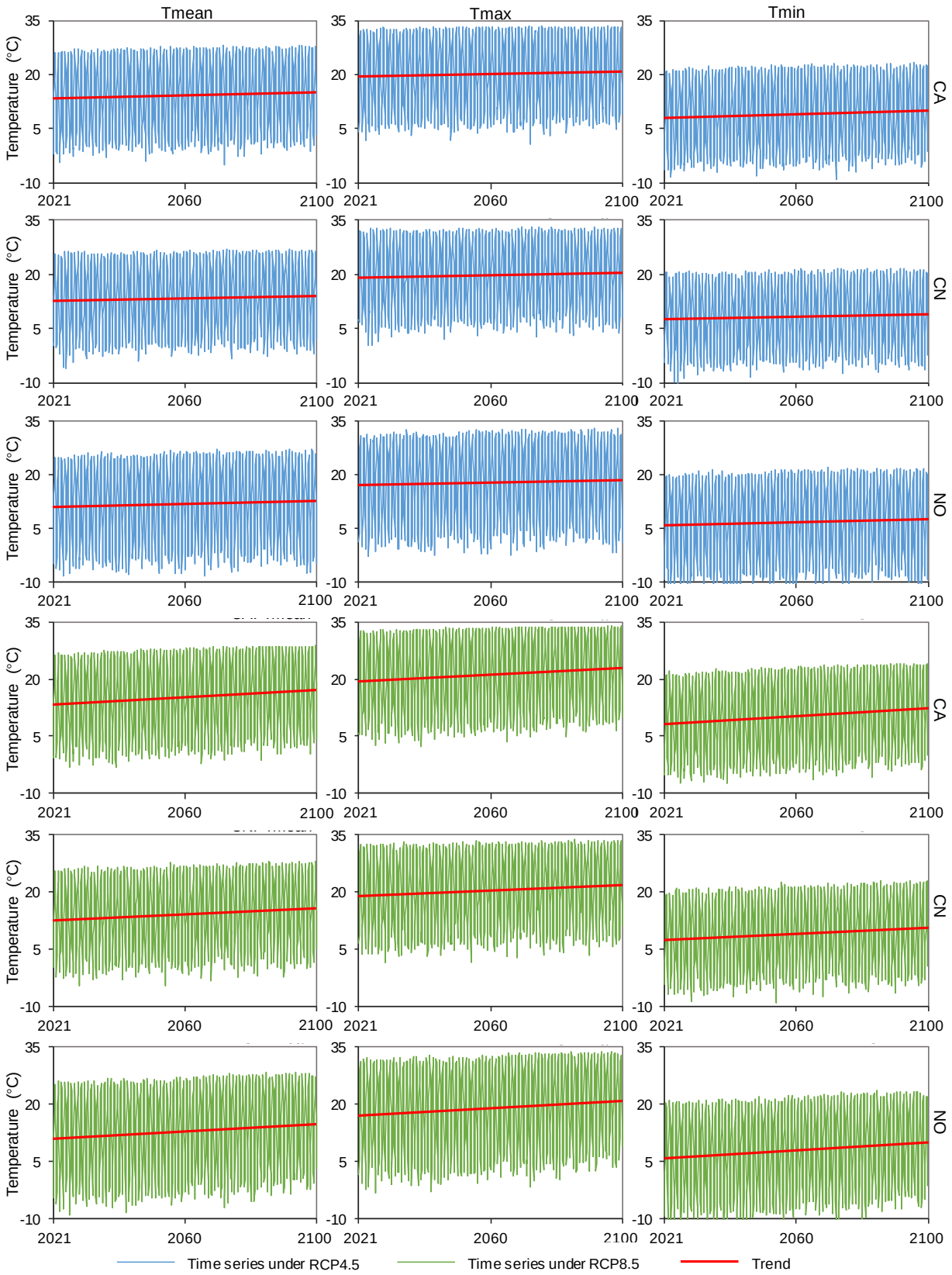

Figure 8. Projected monthly Tmean, Tmax, and Tmin of Hebei (2021 ~ 2100).

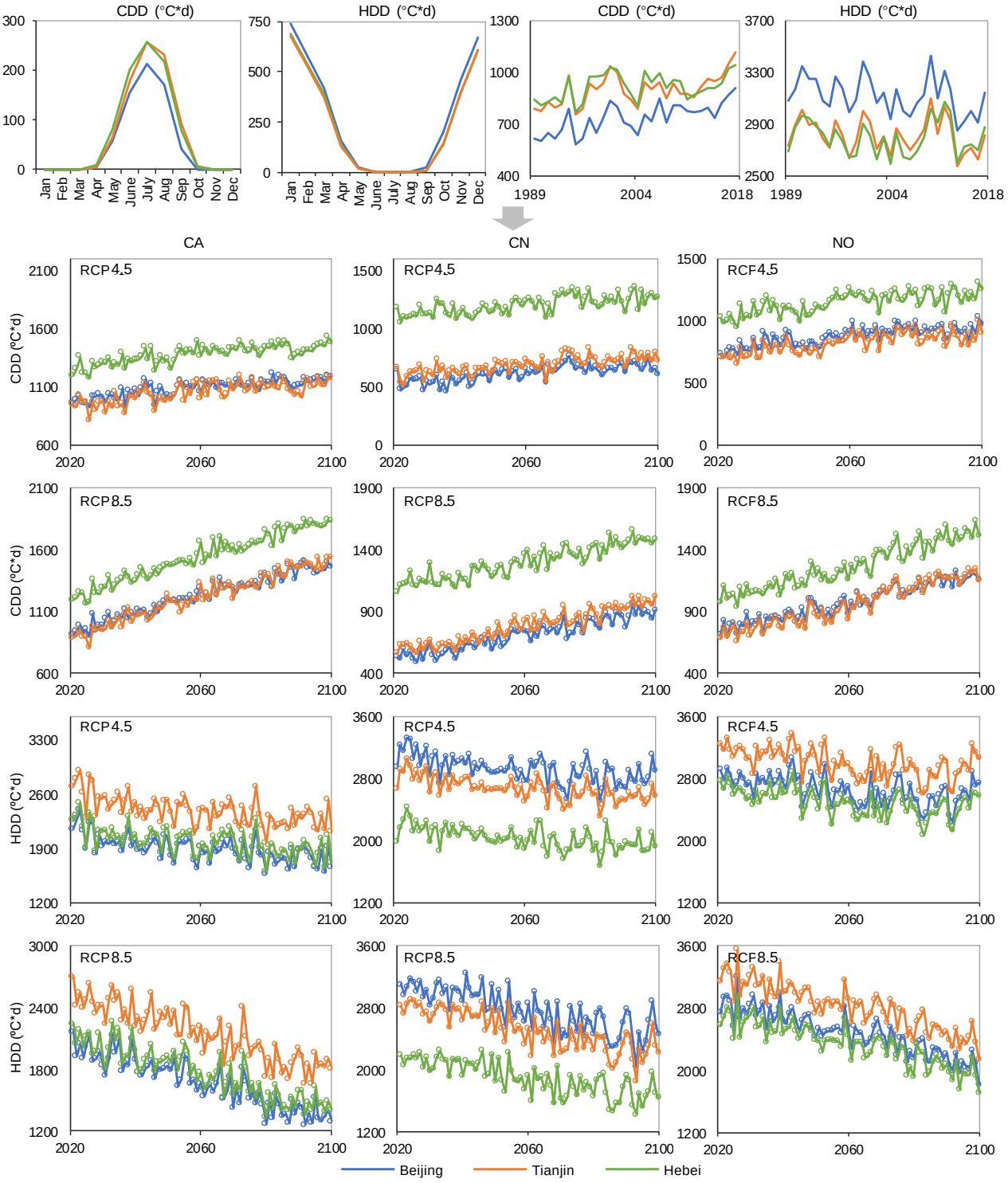

Figure 9. Annual CDD and HDD of Beijing, Tianjin, and Hebei during1989 ~ 2018 and 2021 ~ 2100.

by 0.031 and 0.001%, respectively. When daily Tmean is above 18 °C in one month (usually occurring in winter), 1 °C increase of Tmean can lead to 153 units rising of annual CDD and 4.734% augment of electricity demand; correspondingly, when daily Tmean is below 18 °C in one month (usually occurring in summer), 1 °C decrease of Tmean can bring about annual HDD declining by 212 units and electricity demand decreasing by 0.212%. Apparently, CDD has larger impact on electricity demand than HDD, implying that the hot weather is more sensitive to electricity demand than the cold weather in Jing-Jin-Ji region. This

can be attributed that, for Jing-Jin-Ji region, the heating demand is satisfied by coal (natural gas is the main energy source in winter) and the cooling demand is filled by air conditioning (a large amount of electricity is consumed in summer).

Table 3. Results from the FER Model

Variable	Coefficient	Standard error	t-Statistic	Significance level (p)
HDD	9.87×10^{-5}	3.01×10^{-5}	3.28	0.0023
CDD	3.07×10^{-4}	7.42×10^{-5}	4.14	0.0002
GDP	1.31×10^{-4}	1.03×10^{-5}	12.75	0.0000
RSI	9.21×10^{-3}	2.99×10^{-3}	3.08	0.0039
EI	-1.05×10^{-4}	8.56×10^{-6}	-12.23	0.0000
Constant	25.1	0.17	149.51	0.0000

According to results of the FER model as shown in Table 3, GDP and RSI would also play a positive role but EI would play a negative role in the electricity demand (at 1% significance level). For every 1% GDP growth, electricity demand would increase by 0.013%, demonstrating that economic development can promote electricity demand. Industry produce needs a larger amount of energy, and the proportion of electricity consumption in energy consumption is high in Jing-Jin-Ji region; economy improvement can stimulate people to consume more electricity (e.g., more air conditioning utilization). Besides, 1% increase of RSI can bring about 0.922% increase in electricity demand, indicating the significant pull-effect of secondary industry on electricity demand; this is attributed that the secondary industry is a large consumer of electricity in Jing-Jin-Ji region. On the contrary, every 1% decrease of EI can cause 0.011% increase in electricity demand, revealing that energy efficiency can gradually improve with technology progress and thus lead to electricity demand dropping. Comparing with all factors, the effect of EI on electricity demand would be the highest, indicating that electricity efficiency improvement is important for reducing electricity demand.

4.3. Electricity Demand Prediction

In this study, three GCMs (i.e., CanESM2, CNRM-CM5 and NorESM1-M) and two emission scenarios (RCP4.5 and RCP8.5) were examined, leading to six results for electricity demand prediction. Figure 10 presents results of electricity demand of Jing-Jin-Ji region in 2021 ~ 2100. Regional electricity demand would increase with time under climate change. Compared with the year of 2018, electricity demands of Beijing, Tianjin and Hebei would respectively increase by [108.7, 130.1], [80.4, 114.8] and [206.5, 232.2]% in 2050, and increase by [175.9, 206.6], [47.0, 72.1] and [444.3, 514.7]% in 2100. Among them, electricity-demand increase for Hebei would be the highest, and electricity-demand increase of Tianjin would be the lowest. For the entire region, compared with the year of 2018, electricity demands in 2050 and 2100 would increase by [162.4, 191.6] and [334.9, 391.1]%, respectively.

Different GCMs would lead to varied electricity demand predictions for Jing-Jin-Ji region, as shown in Figure 10. Under RCP4.5, the regional electricity demands (for the future 80 years) would be 142.5×10^{15} (CanESM2), 135.2×10^{15} (CNRM-CM5), and 140.3×10^{15} kWh (NorESM1-M). The largest disparity of annual electricity demand under different GCMs can reach 7.3×10^{15} kWh, about 12.8 times the electricity consumption in 2018. Results demonstrate that the uncertainty of GCMs has significant effect on electricity demand prediction. In 2051 ~ 2100, the electricity demand under RCP8.5 would be higher than that under RCP4.5. For Jing-Jin-Ji region (2021 ~ 2100), the annual electricity demand under RCP8.5 would be [2.3, 5.3] $\times 10^{15}$ kWh, which is about [4.6, 9.4] times the total electricity consumption in 2018. Results demonstrated that climate projections and electricity demand predictions varied significantly across different GCMs and RCPs; projection from one GCM may provide unreliable information for managers, and result in decision-making misplay. Therefore, from a long-term perspective, analyzing the climate change impacts on electricity demand and making adaptive management strategy are important for the sustainable development of electrical power system.

5. Conclusions

In this study, an integrated method (named as MGCMs-SCA-FER) has been developed through incorporating multiple global climate models (MGCMs), stepwise cluster analysis (SCA) and fixed-effects regression (FER) within a general framework. MGCMs-SCA-FER can reflect the inherent uncertainty of GCM, generate high-resolution climate scenarios, quantify climate change impacts, and predict future electricity demand. SCA is capable of handling discrete and nonlinear relationships between predictand and predictor variables; it can downscale large-scale atmosphere simulation outputs from GCMs (predictors) to finer-scale climate projections (predictands). A case study for assessing the impacts of climate change on electricity demand in Jing-Jin-Ji region has been conducted to demonstrate the feasibility of the proposed method. Various climate change projections (time series of minimum, maximum and mean temperatures) of Jing-Jin-Ji region from MGCMs, the impacts assessment of climatic/non-climatic factors on electricity demand, future electricity demand under multiple scenarios were generated. Results demonstrated that the uncertainties of GCMs and RCPs have obvious effects on climate change projections and electricity demand predictions.

The results reveal that: (i) Jing-Jin-Ji region would experience a warmer climate in the next 80 years (for every decade, temperatures rising [0.17, 0.23] °C under RCP4.5 and [0.35, 0.54] °C under RCP8.5); (ii) the projected temperatures from MGCMs would be different, due to the different ways of representing physical processes with different parameterizations in GCMs; (iii) 1 °C increase of temperature would lead to 4.5% augment of annual electricity demand; (iv) electricity intensity has the most significant impact on electricity demand for Jing-Jin-Ji region; (v) electricity demand would increase under all climate scenarios (i.e., electricity demands would increase by [162.4, 191.6]% by 2050 and [334.9, 391.1]% by 2100, compared with the value in 2018); (vi) the electricity demand under RCP8.5 would be higher than that under RCP4.5 by 2100, which is [4.6, 9.4] times the regional electricity consumption in 2018.

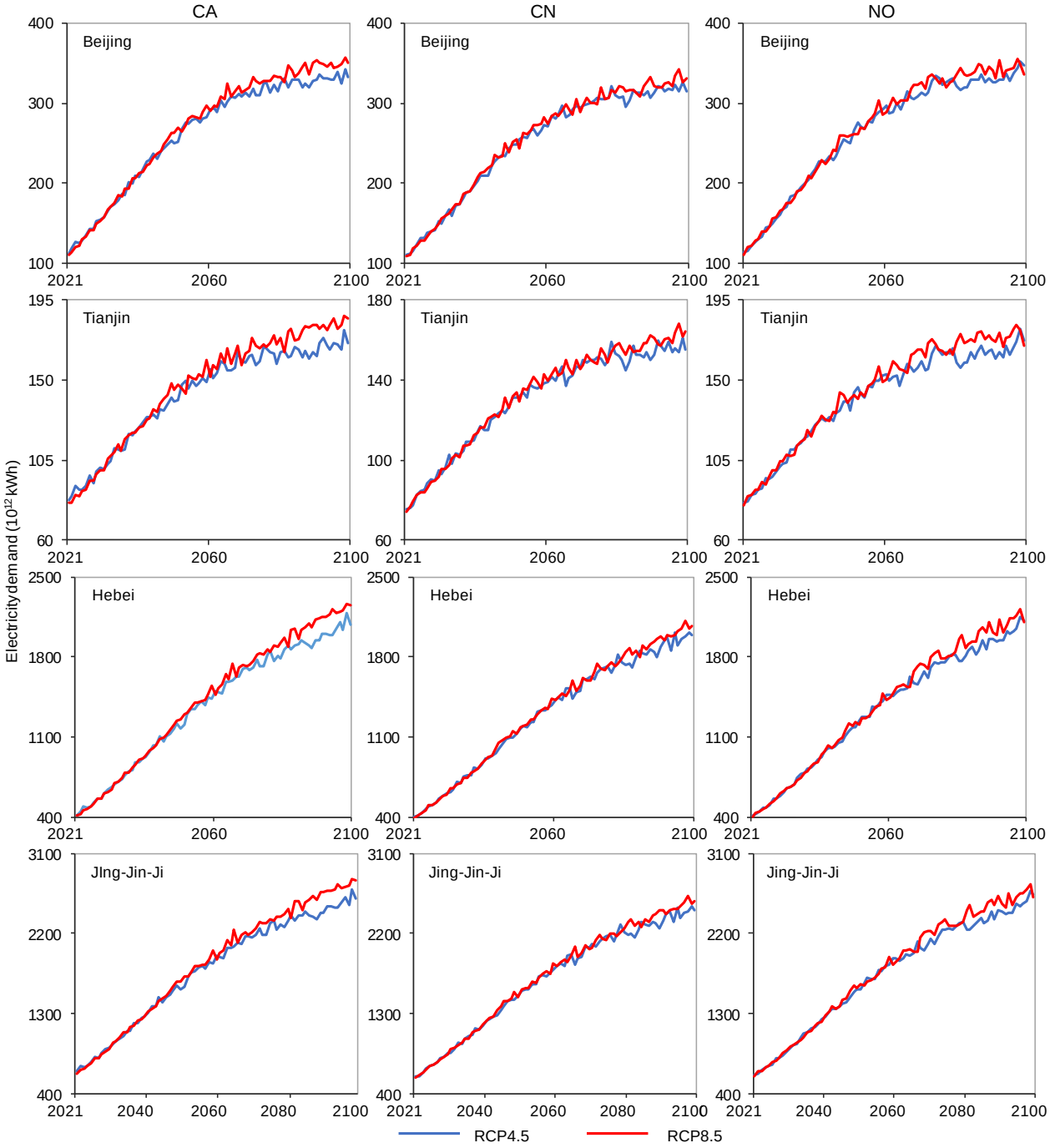

Figure 10. Annual electricity demands of Beijing, Tianjin, and Hebei (2021 ~ 2100).

Both the rapidly socioeconomic development and the intensified global warming would promote the regional electricity demand. If climate change intensifies, the cost and the challenge for electrical power system to adapt to climate change would further intensify; if no effective measure is conducted to abate the global warming, electricity supply in Jing-Jin-Ji region would encounter enormous pressure. Correspondingly, a number of effective measures should be taken to mitigate the impacts of climate change and ensure the security of electricity supply. The most effective way is to improve the efficiency of electricity utilization (especially for Hebei), which can directly relieve the pressure on meeting electricity demand. Besides, developing renewable energy technologies to reduce GHGs emission can contribute to climate change mitigation. Efficient supports of technical, financial and policy are beneficial to stimulating renewable energy utilization.

Appendix: Stepwise cluster analysis

In SCA, sample sets of predictors are cut or merged into new sets, and values of predictands are used as references to judge into which new set a sample in the parent set will enter. In detail, the clustering criterion is the *F* test based on *Wilks'* likelihood ratio criterion. Let cluster *c*, which contains n_c samples, be cut into two sub-clusters *a* and *b* (*a* and *b* contain n_a and n_b samples, respectively, i.e., $n_a + n_b = n_c$). According to *Wilks'* likelihood ratio criterion, if the cutting point is optimal, the value of *Wilks'* Λ ($\Lambda = |U|/|U+V|$) should be the minimum (Kennedy and Gentle, 1981); where *U* and *V* are the total-sample matrix $\{u_{ij}\}$ and the within-groups matrix $\{v_{ij}\}$, respectively; and $|U|$ and $|V|$ mean the determinants of matrixes $\{u_{ij}\}$ and $\{v_{ij}\}$, respectively. When Λ value is very large, clusters *a* and *b* cannot be cut, but must be merged into greater cluster *c*. By Rao's *F*-approximation, the R-statistic can be given by (Rao, 1973; Huang, 1992):

$$R = \frac{1-\Lambda^{1/S}}{\Lambda^{1/S}} \cdot \frac{Z \cdot S - P \cdot (K-1)/2 + 1}{P \cdot (K-1)} \tag{A1}$$

$$Z = n_h - 1 - (P+K)/2 \tag{A2}$$

$$S = \frac{P^2 \cdot (K-1)^2 - 4}{P^2 + (K-1)^2 - 5} \tag{A3}$$

where statistic *R* is distributed approximately as an *F*-variate with $v_1 = P \cdot (K-1)$ and $v_2 = P \cdot (K-1)/2 + 1$ degrees of freedom. *K* is the number of groups, and *P* is the number of predictors. The *R*-statistics can reduce to an exact *F*-variate when *P* = 1 or 2, or when *K* = 2 or 3. Since the number of groups is two (*K* = 2) in this study, an exact *F* test is possible based on the *Wilks'* Λ criterion. Thus, we have $F(P, n_h - P - 1) = (1-\Lambda)/\Lambda \cdot (n_h - P - 1)/P$. The criteria of cutting and merging clusters become to conduct a number of *F*-tests (Rao, 1973). Second step is the tests of optimal cutting points. Sequence n_h samples in cluster *h* according to the values of $x_{r,i}^{(h)}$ in $\{x_i\}$ (r = 1, 2, ..., n). According to *Wilks'* likelihood ratio criterion, the optimal cutting point, which split the cluster *h* into two sub-clusters *e* and *f* when the samples are sequenced according to the values of $x_{r^*,i^*}^{(h)}$ in $\{x_{i^*}\}$, should satisfy that $\Lambda(n_e, n_f)$ is the minimum comparing to that of any other cutting alternatives. Then the *F* test can be undertaken. If (Huang, 1992):

$$F(P', n_e - P' - 1) = \frac{1-\Lambda(n_e, n_f)}{\Lambda(n_e, n_f)} \cdot \frac{n_e - P' - 1}{P'} \geq F_1 \tag{A4}$$

is satisfied, cluster *h* can then be cut into two sub-clusters *e* and *f*. x_{i^*} is identified as the most important predictor, which significantly affects the values of the predictands. Conversely, if Equation (A4) is not satisfied, cluster *h* cannot be cut. Then all the other clusters will be tested and cut if it satisfies the above testing criterion, until no cluster can be further cut. The next step is to test whether any two of the generated sub-clusters should be merged into a new cluster. For two clusters *c* and *d* among the existing *H* clusters, if:

$$F(P', n_c + n_d - P' - 1) = \frac{1-\Lambda(n_c + n_d - 2, 1)}{\Lambda(n_c + n_d - 2, 1)} \cdot \frac{n_c + n_d - P' - 1}{P'} \leq F_2 \tag{A5}$$

is satisfied, clusters *c* and *d* can be merged into a new cluster *g*. Otherwise, If Equation (A5) is not satisfied, clusters *c* and *d* cannot be merged. Then all the other clusters will be tested and merged if it satisfies the above testing criterion, until no clusters can be further merged. Final step is building a cluster tree for prediction. After all calculations and tests have been completed when all hypotheses of further cut or mergence are rejected, a cluster tree can be derived for a new sample prediction (Huang, 1992, 2006).

The predictor values in the cluster tree will be used as the criteria to determine which end nodes the new predictor samples will enter into. The predictands values of the end nodes in the cluster tree will be used to calculate the values of the predictands corresponding to the new predictor samples. Each cutting point, which leads to two branches, corresponds to a value $x_{r^*,i^*}^{(h)}$ of the predictor x_{i^*}. When a new sample set of predictors $\{x_p\}$ is examined, its x_{p,i^*} values are compared with $x_{r^*,i^*}^{(h)}$, at the cutting points and classified into relevant branches. Step-by-step, the sample finally enters in to a tip branch (tip cluster) which cannot be either cut or merged further. Let e' be the tip branch where the new sample enters. Then, the predictands $\{y_p\}$ are (Huang, 1992):

$$y_p = y_p^{(e')} \pm R_p^{(e')} \tag{A6}$$

where $y_p^{(e')}$ is mean of predictor y_p in sub-cluster e', and $R_p^{(e')}$ is radius of y_p in cluster e':

$$y_p^{(e')} = \frac{1}{n}\sum_{k=1}^{n_{e'}} y_{p,k}^{(e')} \quad foralli \tag{A7}$$

$$y_p^{(e')} = \left\{ \max_{k=1}^{n_{e'}}(y_{p,k}^{(e')}) - \min_{k=1}^{n_{e'}}(y_{p,k}^{(e')}) \right\} / 2 \tag{A8}$$

In this study, SCA technique is used for transferring large-scale climate simulation outputs to construct climate change projections at a regional scale.

Acknowledgments. This research was supported by the National Key R&D Program of China (2016YFA0601502) and the Strategic Priority Research Program of Chinese Academy of Sciences (XDA20060302).

References

Ahmed, T., Muttaqi, K.M. and Agalgaonkar, A.P. (2012). Climate change impacts on electricity demand in the State of New South Wales, Australia. *Appl. Energy*, 98(5), 376-383. https://doi.org/10.1016/j.apenergy.2012.03.059

Alberini, A., Prettico, G., Shen, C. and Torriti, J. (2019). Hot weather

and residential hourly electricity demand in Italy. *Energy*, 177, 44-56. https://doi.org/10.1016/j.energy.2019.04.051

AL-Musaylh, M.S., Deo, R.C., Adamowski, J.F. and Li, Y. (2019). Short-term electricity demand forecasting using machine learning methods enriched with ground-based climate and ECMWF reanalysis atmospheric predictors in southeast Queensland, Australia. *Renew. Sustain. Energy Rev*., 113, 109293. https://doi.org/10.1016/j.rser.2019.109293

Ang, B.W., Wang, H. and Ma, X.J. (2017). Climatic influence on electricity consumption: the case of Singapore and Hong Kong. *Energy*, 127, 534-543. https://doi.org/10.1016/j.energy.2017.04.005

Asadoorian, M.O., Eckaus, R.S. and Schlosser, C.A. (2008). Modeling climate feedbacks to electricity demand: the case of China. *Energy Econ.*, 30(4), 1577-1602. https://doi.org/10.1016/j.eneco.2007.02.003

Ayar, P.V., Vrac, M., Bastin, S., Carreau, J., Deque, M. and Gallardo, C. (2016). Intercomparison of statistical and dynamical downscaling models under the EURO- and MED-CORDEX initiative framework: present climate evaluations. *Clim. Dynam*., 46, 1301-1329. https://doi.org/10.1007/s00382-015-2647-5

Beijing Statistical Yearbook 2019. http://data.cnki.net/yearbook/Single/N2019110026

Burillo, D., Chester, M.V., Pincetl, S., Fournier, E.D. and Reyna, J. (2019). Forecasting peak electricity demand for Los Angeles considering higher air temperatures due to climate change. *Appl. Energy*, 236, 1-9. https://doi.org/10.1016/j.apenergy.2018.11.039

Cai, B.F., Mao, X.Q., Wang, J.N. and Wang, M.D. (2019). Fine resolution carbon dioxide emission gridded data and their application for China. *J. Environ. Inform*., 33 (2), 82-95. https://doi:10.3808/jei.201800390

Craig, C.A. and Feng, S. (2016). Exploring utility organization electricity generation, residential electricity consumption and energy efficiency: a climatic approach. *Appl. Energy*, 185, 779-790. https://doi.org/10.1016/j.apenergy.2016.10.101

Dong, C., Huang, G.H., Cai, Y.P. and Liu, Y. (2012). An inexact optimization modeling approach for supporting energy systems planning and air pollution mitigation in Beijing city. *Energy*, 37(1), 673-688. https://doi.org/10.1016/j.energy.2011.10.030

Dong, C., Huang, G.H, and Cheng, G.H. (2021). Offshore wind can power Canada. *Energy*, 121422. https://doi.org/10.1016/j.energy.2021.121422

Emodi, N.V., Chaiechi, T. and Beg, A.R. (2018). The impact of climate change on electricity demand in Australia. *Energy Env.*, 29(7), 1263-1297. https://doi.org/10.1177/0958305X18776538

Empirical Formula. https://tntcat.iiasa.ac.at/SspDb/dsd?Action=htmlpage&page=about (accessed February 12, 2020)

Fan, J.L., Hu, J.W. and Zhang, X. (2019). Impacts of climate change on electricity demand in China: An empirical estimation based on panel data. *Energy*, 170, 880-888. https://doi.org/10.1016/j.energy.2018.12.044

Fu, Y.P., Huang, G.H., Liu, L.R. and Zhai, M.Y. (2021). A factorial CGE model for analyzing the impacts of stepped carbon tax on Chinese economy and carbon emission. *Sci. Total Environ.*, 759, 143512. https://doi.org/10.1016/j.scitotenv.2020.143512

Hebei Economic Yearbook 2018. http://data.cnki.net/yearbook/Single/N2019040177

Hou, Y.J., Xu, H.Q., Yang, Zhao X. and C.Y. (2019). The study case of NorESM1-M on the estimation of spring maize climate potential productivity in northeast China in 2050s. *J. Meteorol. Env.*, 35(4), 100-105. https://doi.org/10.3969/j.issn.1673-503X.2019.04.014

Huang, G.H. (1992). A stepwise cluster analysis method for predicting air quality in an urban environment. *Atmos. Environ. B, Urban Atmos.*, 26(3), 349-357. https://doi.org/10.1016/0957-1272(92)90010-P

Huang, G.H., Huang, Y.F., Wang, G.Q. and Xiao, H.N. (2006). Development of a forecasting system for supporting remediation design and process control based on NAPL biodegradation simulation and stepwise-cluster analysis. *Water Resour. Res*., 42. https://doi.org/10.1029/2005WR004006

Invidiata, A. and Ghisi, E. (2016). Impact of climate change on heating and cooling energy demand in houses in Brazil. *Energy Build*., 130, 20-32. http://doi.org/10.1016/j.enbuild.2016.07.067

IPCC (2013). *Climate Change 2013: The Physical Science Basis. Contribution of Working Group I to the Fifth Assessment Report of the Intergovernmental Panel on Climate Change*. Cambridge University Press, Cambridge, UK, and New York.

Ji, L., Huang, G.H., Niu, D.X., Cai, Y.P. and Yin, J.G. (2020). A stochastic optimization model for carbon-emission reduction investment and sustainable energy planning under cost-risk control. *J. Environ. Inform*., 36 (2), 107-118. https://doi:10.3808/jei.202000428

Jin, S.W., Li, Y.P., Nie, S. and Sun, J. (2017). The potential role of carbon capture and storage technology in sustainable electric-power systems under multiple uncertainties. *Renew. Sustain. Energy Rev*., 80, 467-480. http://dx.doi.org/10.1016/j.rser.2017.05.230

Jylhä, K., Jokisalo, J., Ruosteenoja, K., Pilli-Sihvola, K., Kalamees, T., Seitola, T., Mäkelä H.M., Hyvönen, R., Laapas, M. and Drebs, A. (2015). Energy demand for the heating and cooling of residential houses in Finland in a changing climate. *Energy Build*., 99, 104-116. http://doi.org/10.1016/j.enbuild.2015.04.001

Kennedy, W.J. and Gentle, J.E. (1981). *Statistics: Textbooks and Monograph*s. Marcel Dekker, pp 200-270.

Li, Y.F., Li, Y.P., Huang, G.H. and Chen, X. (2010). Energy and environmental systems planning under uncertainty—an inexact fuzzy-stochastic programming approach. *Appl. Energy*, 87(10), 3189-3211. https://doi.org/10.1016/j.apenergy.2010.02.030

Lv, J., Li, Y.P., Huang, G.H., Suo, C., Mei, H. and Li, Y. (2020). Quantifying the impact of water availability on China's energy system under uncertainties: A perceptive of energy-water nexus. *Renew. Sustain. Energy Rev.*, 134, 110321. https://doi.org/10.1016/j.rser.2020.110321

Mei, H., Li, Y.P., Suo, C., Ma, Y. and Lv, J. (2020). Analyzing the impact of climate change on energy-economy-carbon nexus system in China. *Appl. Energy*, 262, 114568. https://doi.org/10.1016/j.apenergy.2020.114568

Mtongori, H.I., Stordal, F. and Benestad, R.E. (2016). Evaluation of empirical statistical downscaling models' skill in predicting Tanzanian rainfall and their application in providing future downscaled scenarios. *J. Clim*., 29(9), 3231-3252. https://doi.org/10.1175/JCLI-D-15-0061.1

Mukherjee, S., Vineeth, C.R. and Nateghi, R. (2019). Evaluating regional climate-electricity demand nexus: A composite Bayesian predictive framework. *Appl. Energy*, 235, 1561-1582. https://doi.org/10.1016/j.apenergy.2018.10.119

National Bureau of Statistics of the People's Republic of China. China Statistical Yearbook 2018. http://www.stats.gov.cn/tjsj/ndsj/2018/indexch.htm

Perez, J., Menendez, M., Mendez, F.J. and Losada, I.J. (2014). Evaluating the performance of CMIP3 and CMIP5 global climate models over the north-east Atlantic region. *Clim. Dyn*., 43, 2663-2680. https://doi.org/10.1007/s00382-014-2078-8

Physical Science Division of Earth System Research Laboratory. https://www.esrl.noaa.gov/psd/data/gridded/data.ncep.reanalysis.html (accessed January 24, 2020)

Qin, X.S., Huang, G.H. and Chakma, A. (2007). A stepwise-inference-based optimization system for supporting remediation of petroleum-contaminated sites. *Water Air Soil Pollut*., 185, 349-368. https://doi.org/10.1007/s11270-007-9458-1

Rao, C.R. (1973). *Linear Statistical Inference and Its Applications*. Second Editon. Wiley, pp 1-656. https://doi.org/10.1002/9780470316436

Souvignet, M. and Heinrich, J. (2011). Statistical downscaling in the arid central Andes: uncertainty analysis of multi-model simulated

temperature and precipitation. *Theor. Appl. Climatol*., 106, 229-244. https://doi.org/10.1007/s00704-011-0430-z

Su, Y.Y., Li, Y.P., Huang, G.H., Jia, Q.M. and Li, Y.F. (2021). An integrated multi-GCMs Bayesian-neural-network hydrological analysis method for quantifying climate change impact on runoff of the Amu Darya River basin. *Int. J. Climatol*., 41, 3411-3424. https://doi.org/10.1002/joc.7026

Sun, J., Li, Y.P., Suo, C. and Huang, G.H. (2019). Identifying changes and critical drivers of future temperature and precipitation with a hybrid stepwise-cluster variance analysis method. *Theor. Appl. Climatol*., 137, 2437-2450. https://doi.org/10.1007/s00704-018-02758-9

Tianjin Statistical Yearbook 2018. http://data.cnki.net/yearbook/Single/N2019030264

Wang, X.Q., Huang, G.H., Lin, Q.G., Nie, X.H., Cheng, G.H., Fan, Y.R., Li, Z., Yao, Y. and Suo, M.Q. (2013). A stepwise cluster analysis approach for downscaled climate projection—a Canadian case study. *Environ. Model. Softw*., 49, 141-151. https://doi.org/10.1016/j.envsoft.2013.08.006

Yaffee, B.R. (2003). A primer for panel data analysis. https://www.researchgate.net/publication/266417453

Zeng, Y., Cai, Y., Huang, G.H. and Dai, J. (2011). A review on optimization modeling of energy systems planning and GHG emission mitigation under uncertainty. *Energies*, 4(10), 1624-1656. https://doi.org/10.3390/en4101624

Zhai, M.Y., Huang, G.H., Liu, L.R., Zheng, B.Y. and Guan, Y.R. (2020). Inter-regional carbon flows embodied in electricity transmission: network simulation for energy-carbon nexus. *Renew. Sustain. Energy Rev.*, 118, 109511. https://doi.org/10.1016/j.rser.2019.109511

Zhai, Y.Y., Huang, G.H., Wang, X.Q., Zhou, X., Lu, C. and Li, Z. (2019). Future projections of temperature changes in Ottawa, Canada through stepwise clustered downscaling of multiple GCMs under RCPs. *Clim. Dyn*., 52, 3455-3470. https://doi.org/10.1007/s00382-018-4340-y

Zheng, S.G., Huang, G.H., Zhou, X. and Zhu, X.H. (2020). Climate-change impacts on electricity demands at a metropolitan scale: A case study of Guangzhou, China. *Appl. Energy*, 261. 114295. https://doi.org/10.1016/j.apenergy.2019.114295

Zhou, X., Huang, G.H., Wang, X.Q., Fan, Y.R. and Cheng, G.H. (2018). A coupled dynamical-copula downscaling approach for temperature projections over the Canadian Prairies. *Clim. Dyn*., 51(7), 2413-2431. https ://doi.org/10.1007/s0038 2-017-4020-3

Zhuang, X.W., Li, Y.P., Huang, G.H. and Wang, C.X. (2017). Evaluating climate change impacts on the hydrology of watershed in northwestern China using a stepwise-clustered downscaling approach. *Int. J. Climatol*., 37, 2961-2976. https://doi.org/10.1002/joc.4892

Zhuang, X.W., Li, Y.P., Nie, S., Fan, Y.R. and Huang, G.H. (2018). Analyzing climate change impacts on water resources under uncertainty using an integrated simulation-optimization approach. *J. Hydrol*., 556, 523-538. https://doi.org/10.1016/j.jhydrol.2017.11.016